Electronic Supplementary Material (ESI) for Physical Chemistry Chemical Physics.

Supporting Information

A theoretical study on novel orthorhombic group-ⅣB nitride halides monolayers for photocatalytic overall water splitting

Jiali Wang, [a] Jiajun Lu, [a] Xiuwen Zhao, [a] Guichao Hu, [a] Xiaobo Yuan, [a] Siyun Qi*[a] and Junfeng Ren*[ab]

[a] School of Physics and Electronics, Shandong Normal University, Jinan, 250358, China.

[b] Shandong Provincial Engineering and Technical Center of Light Manipulations & Institute of Materials and Clean Energy, Shandong Normal University, Jinan 250358, China.

Supporting Figures

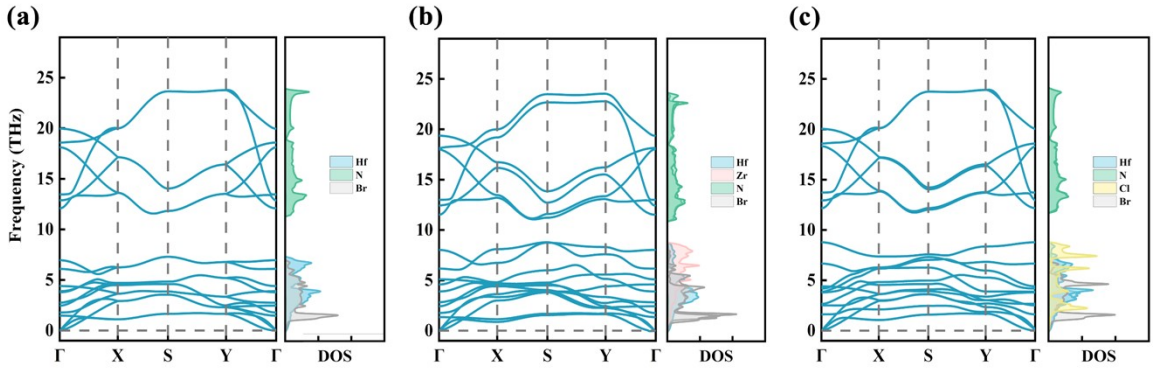

Fig. S1 Phonon dispersion curves and phonon DOS for (a) $Hf_2N_2Br_2$, (b) $HfZrN_2Br_2$ and (c) Hf_2N_2ClBr monolayers.

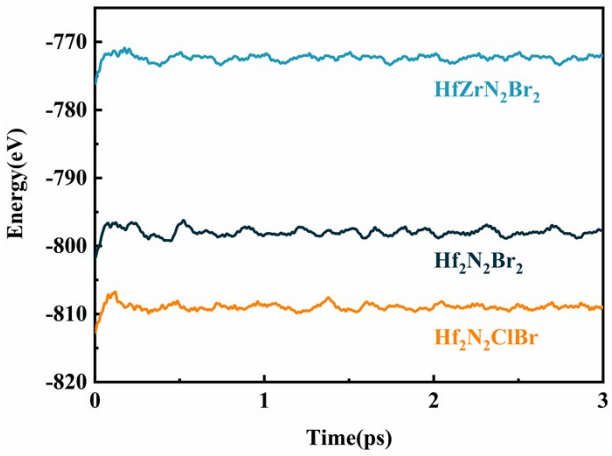

Fig. S2 The total potential energies in the AIMD simulation at 300K for 3 ps.

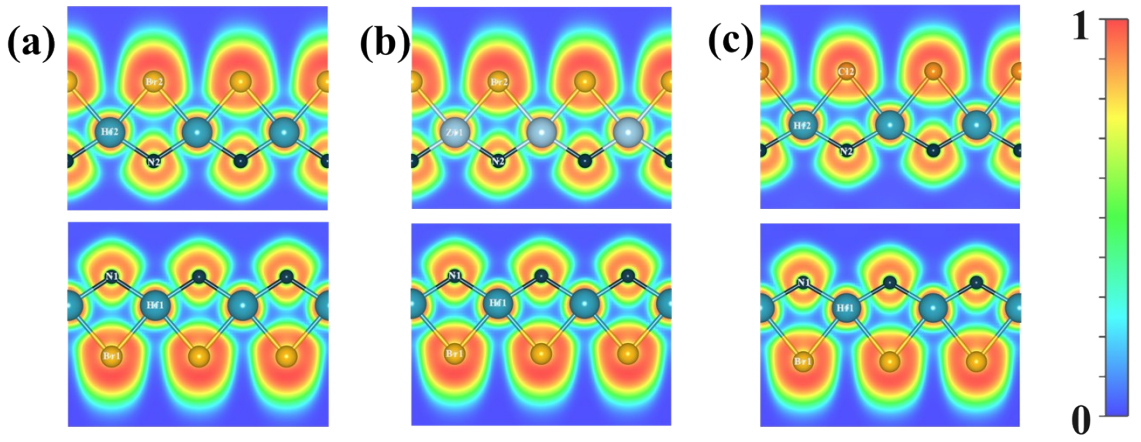

Fig. S3 The electron localization function (ELF) for (a) $Hf_2N_2Br_2$, (b) $HfZrN_2Br_2$ and (c) Hf_2N_2ClBr monolayers. The values of vertical bar represent the localized level of electrons. The values of 0 and 1 represent low electron density and fully localized electron region, respectively.

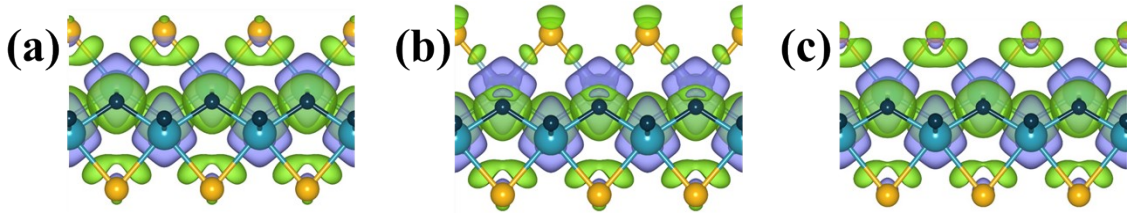

Fig. S4 The charge density difference for (a) $Hf_2N_2Br_2$, (b) $HfZrN_2Br_2$ and (c) Hf_2N_2ClBr monolayers. The light purple and green colors represent the charge depletion and accumulation on the surface of 0.006 $eÅ^{-3}$, respectively.

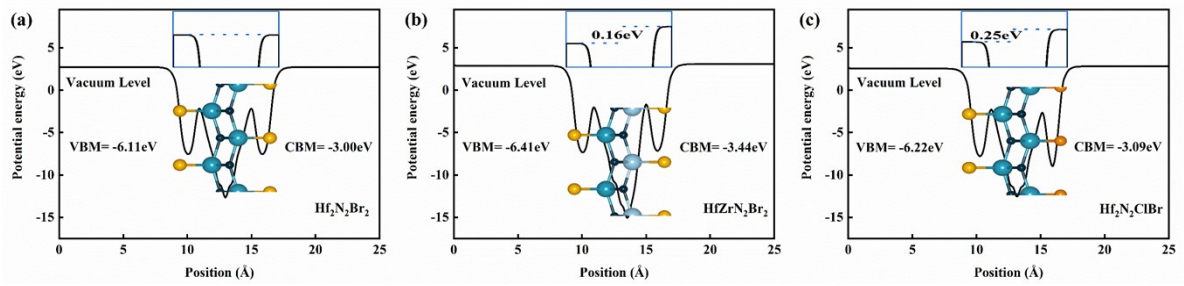

Fig. S5 The plane-averaged electrostatic potentials for (a) $Hf_2N_2Br_2$, (b) $HfZrN_2Br_2$ and (c) Hf_2N_2ClBr monolayers. The insets show the electrostatic potential difference.

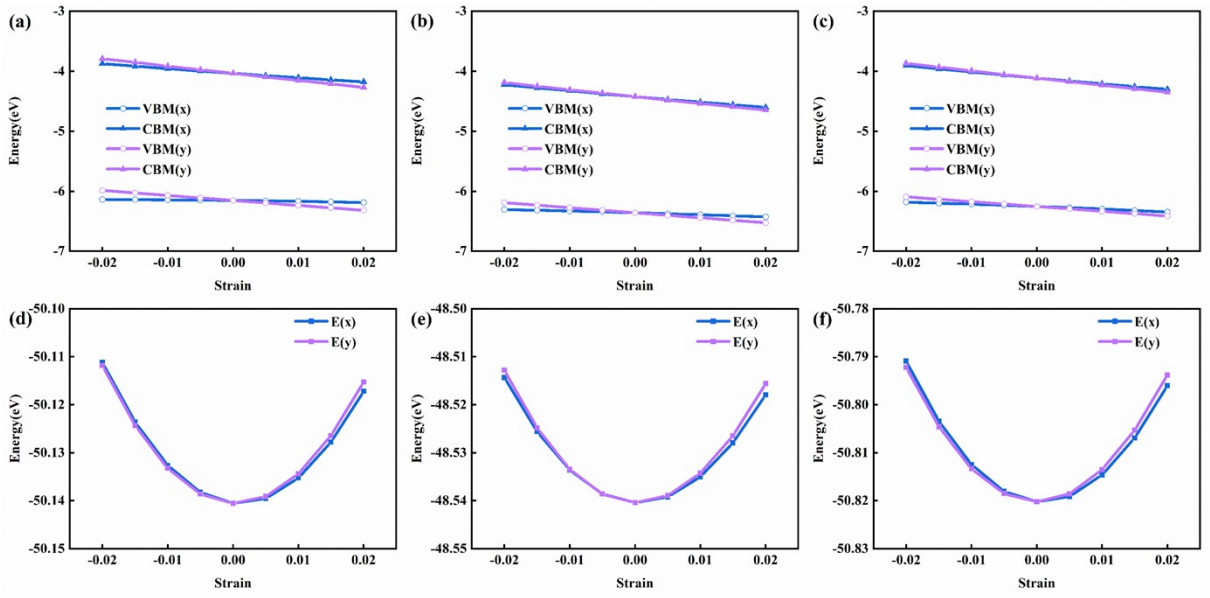

Fig. S6 The band edge positions for (a) $Hf_2N_2Br_2$, (b) $HfZrN_2Br_2$, and (c) Hf_2N_2ClBr monolayers under uniaxial strain along different directions, and the corresponding energies are shown in (d), (e), and (f).

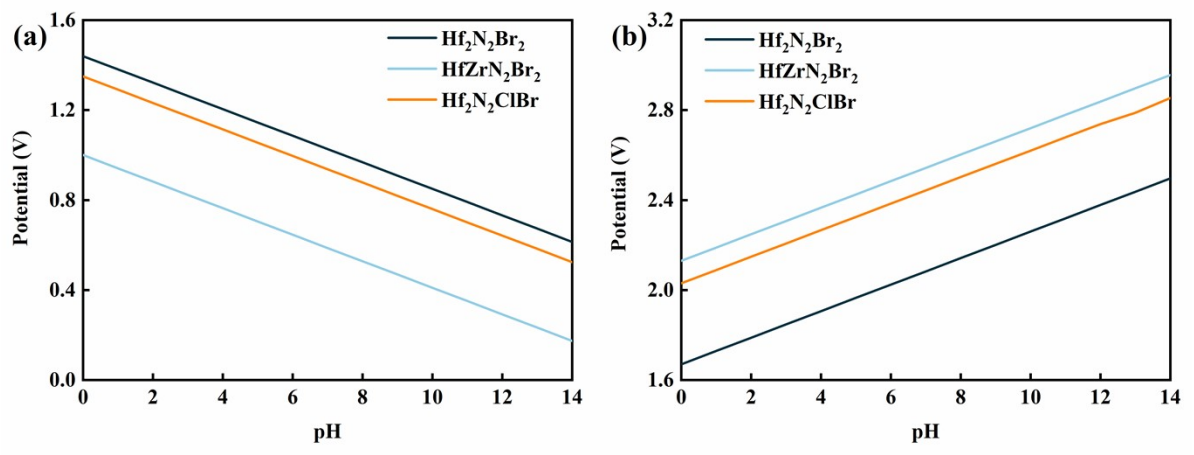

Fig. S7 The external potentials provided by (a) U_e and (b) U_h at different pH for $Hf_2N_2Br_2$, Janus $HfZrN_2Br_2$ and Janus Hf_2N_2ClBr monolayers, respectively.

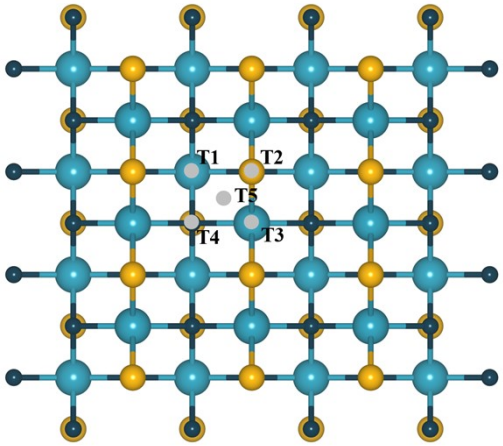

Fig. S8 The different adsorption sites considered for $Hf_2N_2Br_2$, Janus $HfZrN_2Br_2$ and Janus Hf_2N_2ClBr monolayers, respectively. Here, Tn (n=1-5) are the five different adsorption sites. And the gray colors represent different adsorbates (H^*, OH^*, O^* and OOH^*).

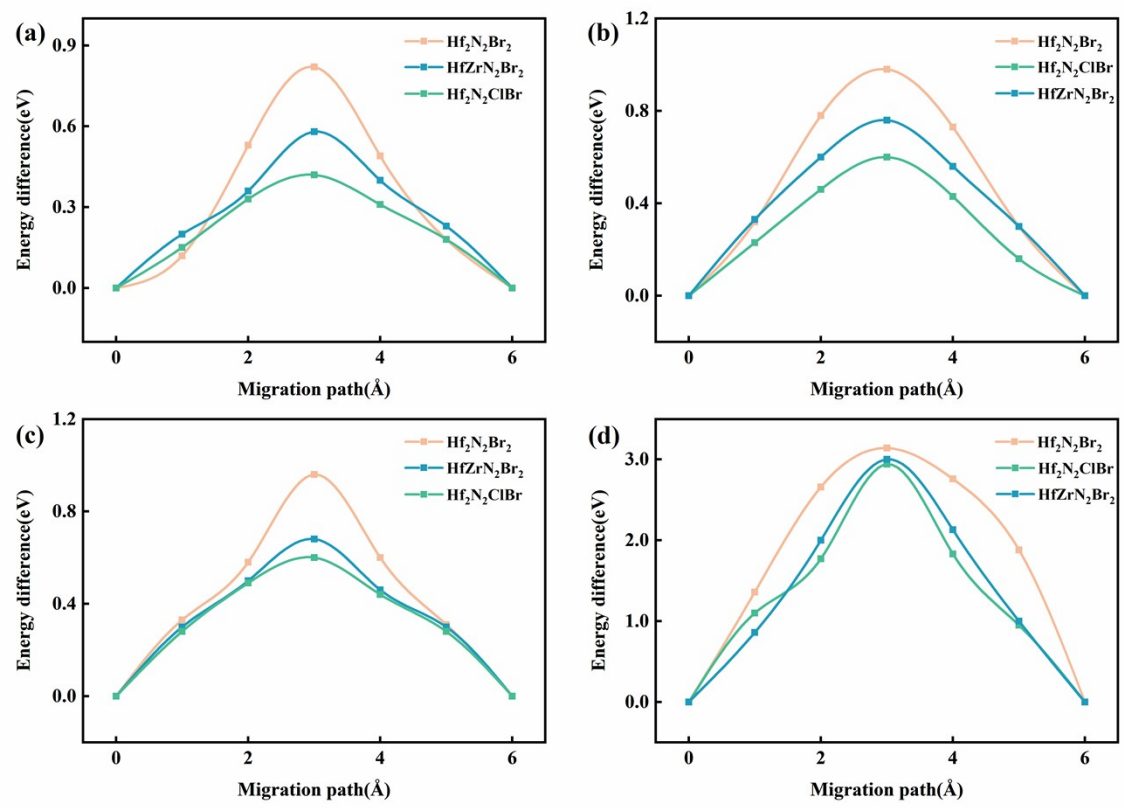

Fig. S9 The corresponding energy difference for (a) H^*, (b) OH^*, (c) O^* and (d) OOH^* along different migration paths.

Species	View	$Hf_2N_2Br_2$	$HfZrN_2Br_2$	Hf_2N_2ClBr
H^*	Top view	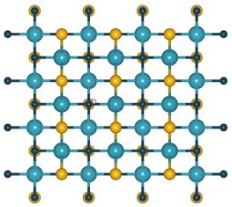	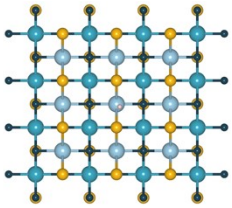	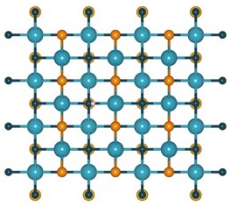
	Side view	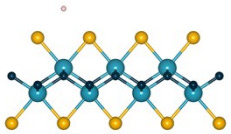	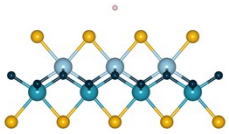	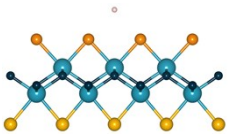
OH^*	Top view	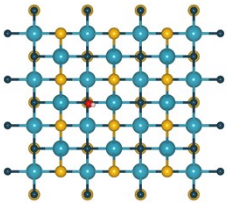	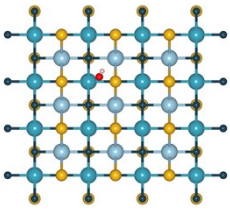	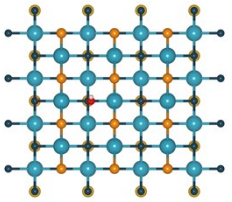
	Side view	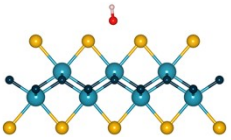	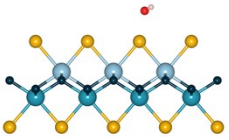	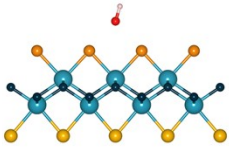
O^*	Top view	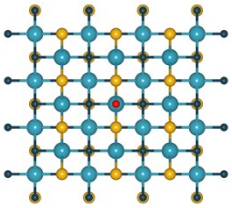	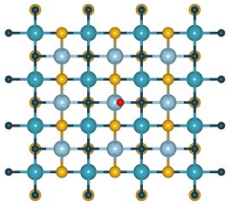	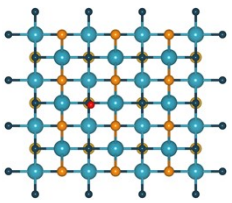
	Side view	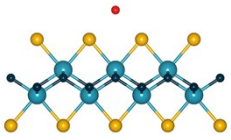	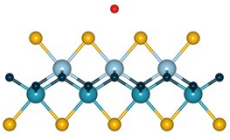	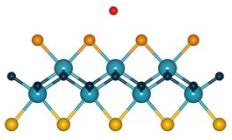

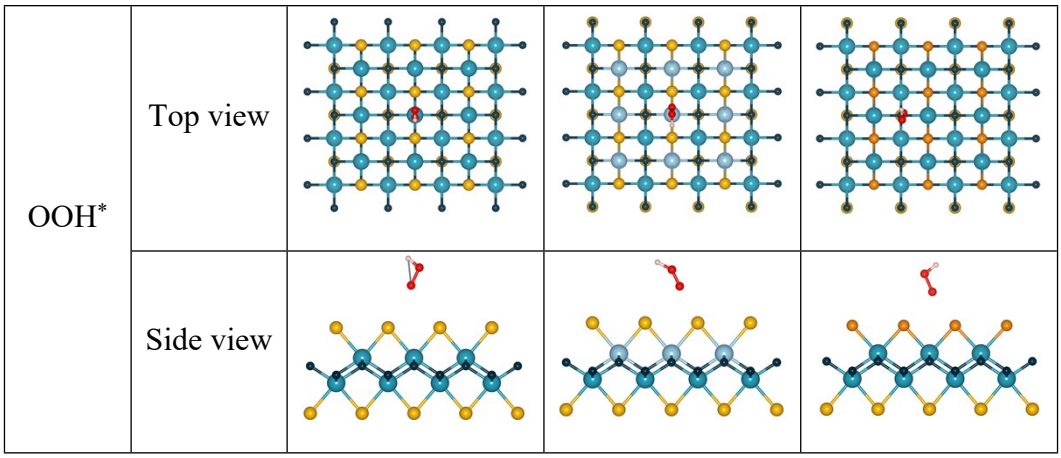

Fig. S10 The top view and side view of relaxed structure after adsorption of H^*, OH^*, O^* and OOH^*, respectively.

Supporting Tables

Table S1 The calculated band gaps (E_g^{PBE} and E_g^{HSE}) using PBE and HSE methods, formation energy (E_f), work function (W_1 and W_2), electrostatic potential difference (ΔW), valence band potential (E_{VBM}), conduction band potential (E_{CBM}) for $Hf_2N_2Br_2$, Janus $HfZrN_2Br_2$ and Janus Hf_2N_2ClBr monolayers.

material	E_g^{PBE} (eV)	E_g^{HSE} (eV)	E_f (eV)	W_1 (eV)	W_2 (eV)	ΔW (eV)	E_{VBM} (eV)	E_{CBM} (eV)
$Hf_2N_2Br_2$	2.12	3.11	-3.39	2.70	2.70	0	-6.11	-3.00
$HfZrN_2Br_2$	1.93	2.97	-3.31	2.89	3.05	0.16	-6.41	-3.44
Hf_2N_2ClBr	2.14	3.13	-3.49	2.53	2.78	0.25	-6.22	-3.09

Table S2 The Bader charge analysis for (a) $Hf_2N_2Br_2$, (b) $HfZrN_2Br_2$ and (c) Hf_2N_2ClBr monolayers. Negative and positive values represent charge loss and gain.

$Hf_2N_2Br_2$		$HfZrN_2Br_2$		Hf_2N_2ClBr	
Br2	+0.603	Br2	+0.615	Cl1	+0.662
Hf2	-2.256	Zr1	-2.252	Hf2	-2.315
N2	+1.653	N2	+1.640	N2	+1.657
N1	+1.653	N1	+1.644	N1	+1.658
Hf1	-2.256	Hf1	-2.253	Hf1	-2.271
Br1	+0.603	Br1	+0.606	Br1	+0.609

Table S3 The adsorption energy of H* adsorbed at different adsorption sites.

material	surface	T1	T2	T3	T4	T5
$Hf_2N_2Br_2$	Br	-0.48	-0.83	-0.33	-1.26	-0.90
$HfZrN_2Br_2$	Br(top)	-0.72	-0.38	-0.92	-0.62	-0.66
	Br(bottom)	-0.88	-0.65	-0.49	-0.53	-0.54
Hf_2N_2ClBr	Cl(top)	-0.66	-0.33	-0.84	-0.58	-0.68
	Br(bottom)	-0.73	-0.44	-0.62	-0.68	-0.63

Table S4 The adsorption energy of OH^* adsorbed at different adsorption sites.

material	surface	T1	T2	T3	T4	T5
$Hf_2N_2Br_2$	Br	-1.40	-0.33	-0.33	-0.26	-0.90
$HfZrN_2Br_2$	Br(top)	-1.02	-0.38	-0.66	-0.72	-0.66
	Br(bottom)	-0.98	-0.45	-0.49	-1.13	-0.54
Hf_2N_2ClBr	Cl(top)	-0.16	-0.13	-0.14	-0.98	-0.68
	Br(bottom)	-0.13	-0.44	-0.32	-0.78	-0.63

Table S5 The adsorption energy of O^* adsorbed at different adsorption sites.

material	surface	T1	T2	T3	T4	T5
$Hf_2N_2Br_2$	Br	-0.70	-0.33	-1.66	-0.56	-0.90
$HfZrN_2Br_2$	Br(top)	-1.02	-0.38	-1.23	-1.00	-0.66
	Br(bottom)	-0.98	-0.45	-0.49	-1.03	-0.54
Hf_2N_2ClBr	Cl(top)	-0.76	-0.53	-0.74	-1.01	-0.68
	Br(bottom)	-0.63	-0.44	-0.32	-0.98	-0.63

Table S6 The adsorption energy of OOH^* adsorbed at different adsorption sites.

material	surface	T1	T2	T3	T4	T5
$Hf_2N_2Br_2$	Br	-2.01	-0.33	-2.86	-0.86	-0.90
$HfZrN_2Br_2$	Br(top)	-1.02	-0.38	-1.76	-1.32	-0.66
	Br(bottom)	-0.98	-0.45	-0.49	-1.13	-0.54
Hf_2N_2ClBr	Cl(top)	-0.76	-1.13	-1.14	-1.68	-0.68
	Br(bottom)	-1.13	-0.44	-1.32	-0.98	-0.63

Calculation details

The photocatalytic water splitting reactions happen in solution, so the calculations are performed using VASPsol considering the solvation effect. The equation is as follows:

$$E_{sol} = E_{tot;sol} - E_{tot;vac}$$

where $E_{tot;sol}$ and $E_{tot;vac}$ represent the vacuum state energy and the solvation state energy, respectively. The details are shown as follows:

	$E_{tot;sol}$	$E_{tot;vac}$	E_{sol}
$Hf_2N_2Br_2$	-50.149	-50.143	-0.006
$HfZrN_2Br_2$	-50.326	-50.249	-0.077
Hf_2N_2ClBr	-50.841	-50.830	-0.011

Since the geometry is periodic in the (x, y) plane, the planar average is considered as a function of the z-coordinate only. Based on the three-dimensional electron charge density, we can obtain the average one-dimensional electrostatic potential $\bar{V}(z)$ by calculating the planar average function $\bar{f}$[1]:

$$\bar{f}(z) = \frac{1}{S}\int_S V(r)dxdy$$

where S represents the area of a unit cell in the x-y plane.

The external potentials provided by the photogenerated electrons (U_e) and photogenerated holes (U_h) in the photocatalyst are defined as[2]:

$$U_e = \left|E_{CBM} - E_{H^+/H_2}\right|/e$$

$$U_h = \left|E_{VBM} - E_{H^+/H_2} + \Delta W\right|/e$$

In an aqueous solution, the photocatalytic water splitting reaction is composed by the following two half-reactions.

According to the approach proposed by Norskov, the Gibbs free energy difference (ΔG) is described as[3-7]:

$$\Delta G = \Delta E + \Delta E_{ZPE} - T\Delta S - eU + 0.059 \times pH$$

where ΔE, ΔE_{ZPE}, and ΔS represent the energy difference of adsorption, zero-point energy and entropy, respectively. The energies of ΔE and ΔE_{ZPE} are obtained by DFT calculations, and the value for ΔS is obtained via the standard thermodynamic data. Furthermore, T, e and U are the system temperature (298 K), the charge of electron and the potential relative to the reduction potential of H^+/H_2. We calculate ΔG for the three monolayers using the 3×3×1 supercell, which avoids the interaction of adjacent adsorbed atoms.

References:

1. M. Peressi, N. Binggeli and A. Baldereschi, *J. Phys. D: Appl. Phys.*, 1998, **31**, 1273.
2. Y. Yu, J. Zhou, Z. Guo and Z. Sun, *ACS Appl. Mater. Interfaces*, 2021, **13**, 28090-28097.
3. X. Gao, Y. Zhou, Y. Tan, B. Yang, Z. Cheng and Z. Shen, *Int. J. Hydrog. Energy*, 2019, **44**, 14861-14868.
4. S. Qi, Y. Fan, J. Wang, X. Song, W. Li and M. Zhao, *Nanoscale*, 2020, **12**, 306-315.
5. Q. Yang, H. Liu, P. Yuan, Y. Jia, L. Zhuang, H. Zhang, X. Yan, G. Liu, Y. Zhao, J. Liu, S. Wei, L. Song, Q. Wu, B. Ge, L. Zhang, K. Wang, X. Wang, C. R. Chang and X. Yao, *J. Am. Chem. Soc.*, 2022, **144**, 2171-2178.
6. Y. Guo, L. Mao, Y. Tang, Q. Shang, X. Cai, J. Zhang, H. Hu, X. Tan, L. Liu, H. Wang, T. Yu and J. Ye, *Nano Energy*, 2022, **95**, 107028.
7. S. Qi, J. Wang, X. Song, Y. Fan, W. Li, A. Du and M. Zhao, *Sci. Bull.*, 2020, **65**, 995-1002.